Study of the optimal duty cycle and pumping rate for square-wave amplitude-modulated Bell–Bloom magnetometers*

Mei-Ling Wang(王美玲)[1,2], Meng-Bing Wang(王梦冰)[1,2], Gui-Ying Zhang(张桂迎)[1,2], and Kai-Feng Zhao(赵凯锋)[1,2,†]

[1] *Applied Ion Beam Physics Laboratory, Key Laboratory of the Ministry of Education, Fudan University, Shanghai* 200433, *China*

[2] *Institute of Modern Physics, Department of Nuclear Science and Technology, Fudan University, Shanghai* 200433, *China*

(Received 4 December 2015; revised manuscript received 4 February 2016; published online 20 April 2016)

We theoretically and experimentally study the optimal duty cycle and pumping rate for square-wave amplitude-modulated Bell–Bloom magnetometers. The theoretical and the experimental results are in good agreement for duty cycles and corresponding pumping rates ranging over 2 orders of magnitude. Our study gives the maximum field response as a function of duty cycle and pumping rate. Especially, for a fixed duty cycle, the maximum field response is obtained when the time averaged pumping rate, which is the product of pumping rate and duty cycle, is equal to the transverse relaxation rate in the dark. By using a combination of small duty cycle and large pumping rate, one can increase the maximum field response by up to a factor of 2 or $\pi/2$, relative to that of the sinusoidal modulation or the 50% duty cycle square-wave modulation respectively. We further show that the same pumping condition is also practically optimal for the sensitivity due to the fact that the signal at resonance is insensitive to the fluctuations of pumping rate and duty cycle.

Keywords: optical pumping, spin relaxation, power-broadening, magnetometry

PACS: 07.55.Ge, 32.80.Xx, 76.60.Es, 76.70.Hb **DOI:** 10.1088/1674-1056/25/6/060701

1. Introduction

The principle of Bell–Bloom magnetometer (BBM) is based on the discovery of Bell and Bloom in 1961, that the precession of atomic ground state polarization at Larmor frequency can be induced by synchronous amplitude-modulation (AM) of the optical pumping light with either circular[1] or linear[2] polarization. This technology was soon used in magnetometry and various versions of the BBM have been developed,[3–7] including frequency-[8,9] and polarization-modulation.[10–12]

The precession of the atomic polarization can be measured by transmission of circular polarized light as well as nonlinear magneto-optical rotation (paramagnetic Faraday rotation) of linearly polarized light.[13] Very high signal-to-noise ratio can be achieved by phase-sensitive detection referenced to the 1st or higher harmonics of the modulation frequency. It is often practical and convenient to pump and probe with a single beam. However, two-beam scheme has the advantage of allowing the separate study and optimization of the pumping and probing processes.[14] Pustelny *et al.* studied AM BBM using a single linearly polarized beam for different light intensities, duty cycles and modulation wave forms.[15] Schultze *et al.* compared the characteristics and performance of the *M*–*x* magnetometer with those of the AM BBM for different duty cycles and modulation depths.[16] Grujic and Weis modeled and partially verified the magnetic resonance signals occurring in amplitude-, frequency-, and polarization-modulated light for the single-beam scheme.[17] In those studies the pumping rate was much smaller than the transverse relaxation rate in the dark Γ_2 and power broadening was neglected. Compared with sinusoidal AM whose pumping-rate effect was well studied,[18] square-wave AM has an extra control parameter, the duty cycle, allowing further tweaking the performance of the magnetometer. In this article we theoretically and experimentally analyze the effects of the pumping rate and the modulation duty cycle on the field response and the noise of the system. While most previous studies used pumping rates smaller than or comparable to Γ_2 and duty cycles on the order of several tens of percent, our study covers a range of duty cycles and corresponding pumping rates over 2 orders of magnitude. We find that, using a small duty cycle while keeping the time averaged pumping rate close to Γ_2, we can increase the field response of magnetometer at resonance by up to a factor of $\pi/2$ comparing to the common case of 50% duty cycle. The sensitivity is also optimized in the same condition since the fluctuation of pumping parameters has virtually no effect on the field response at resonance.

2. Theory

We assume that a vapor cell containing alkali atoms with gyromagnetic ratio γ is placed in a static magnetic field B_0 along the z direction corresponding to a Larmor frequency $\omega_0 = \gamma B_0$. The atoms are optically pumped by a circularly polarized beam in the x direction whose intensity is modulated by a square wave with 100% modulation depth. The atomic spin polarization is detected by a linearly polarized

*Project supported by the National Natural Science Foundation of China (Grant No. 11074050).

†Corresponding author. E-mail: zhaokf@fudan.edu.cn

© 2016 Chinese Physical Society and IOP Publishing Ltd

probe beam along the y axis using paramagnetic Faraday rotation (PFR) method, the signal of which is due primarily to the magnetic dipole moment (MDM) of the atomic ensemble along the beam direction.[19,20] We also assume that ω_0 is much smaller than the linewidths of the pump and the probe light. If we define

$$M_+ \equiv M_x + \mathrm{i}M_y, \tag{1}$$

where M_x and M_y are the x and y components of the MDM respectively, the Bloch equations for M_x and M_y can be combined into a single complex equation:

$$\frac{\mathrm{d}M_+}{\mathrm{d}t} = -\mathrm{i}\omega_0 M_+ - M_+\left[\Gamma_2 + R\right] + RM_0, \tag{2}$$

where $R(t)$ is the optical pumping rate associated with the MDM and M_0 is the equilibrium MDM that can be pumped in the absence of B_0 and Γ_2,

The square-wave amplitude-modulation of the pump beam is assumed to be symmetrical about the time zero without loss of generality, so that the Fourier series expansion of $R(t)$ contains only cosine terms as shown below.

$$R(t) = R_0 d + \sum_{n=1}^{\infty} \frac{2R_0}{n\pi} \sin(n\pi d)\cos(n\omega t), \tag{3}$$

where R_0 is the amplitude of the square-wave of the pumping rate, ω is the modulation frequency and d is the modulation duty cycle. To obtain an analytical solution of Eq. (2) by Fourier expansion, we need to make two simplifications. 1) Γ_2 is time independent. In a typical alkali metal vapor cell, $\Gamma_2 = \Gamma_{\mathrm{SE}} + \Gamma_{\mathrm{SD}} + \Gamma_{\mathrm{W}}$, where Γ_{SE} and Γ_{SD} are respectively, the relaxation rate due to spin exchange collisions and spin destruction collisions, and Γ_{W} represents the total rate of other relaxation mechanisms such as atom-wall collisions and atom loss to reservoir. Because spin exchange collisions conserve the total spin of the interacting atoms, Γ_{SE} is a function of the total spin polarization $|M_+|$, hence time dependent, which makes Eq. (2) nonlinear. However, if $\Gamma_{\mathrm{SE}} \ll \Gamma_{\mathrm{W}}$, it can be neglected and Γ_2 becomes a constant of time; or if $\Gamma_2 \ll \omega$, then the variation of $|M_+|$ will be negligible in the final steady state which makes Γ_{SE} and Γ_2 approximately constant also. 2) $\overline{R(t)} \ll \omega$. Owing to the product term $M_+(t)R(t)$, coefficients of different harmonics recursively couple with each other to infinitely large orders. However, if time averaged $R(t)\overline{R(t)}$, is much smaller than the modulation frequency, one can replace $R(t)$ by $\overline{R(t)}$.[21] Under these two conditions, the coefficient of the 2nd term of M_+ in Eq. (2) becomes a constant given by

$$\Gamma_2(t) + R(t) \approx \Gamma_2 + \overline{R(t)} = \Gamma_2 + R_0 d \equiv \Gamma, \tag{4}$$

where Γ can be regarded as the total transverse relaxation rate. Substituting Eqs. (4) and (3) into Eq. (2), we have

$$\frac{\mathrm{d}M_+}{\mathrm{d}t} + \mathrm{i}\omega_0 M_+ + \Gamma M_+ = M_0\left[R_0 d + \sum_{n=1}^{\infty} \frac{2R_0}{n\pi}\sin(n\pi d)\cos(n\omega t)\right]. \tag{5}$$

To obtain the steady state solution of Eq. (5), we expand M_+ by Fourier series

$$M_+ = \sum_{n=-\infty}^{+\infty} M_+^{(n)} \exp(-\mathrm{i}n\omega t), \tag{6}$$

where $M_+^{(n)}$'s are the time independent amplitudes. For Eq. (5) to hold true, the coefficients for harmonics of the same order on both side of the equation must be equal. Therefore $M_+^{(n)}$ is

$$M_+^{(n)} = \frac{M_0 R_0 d\,\mathrm{sinc}(n\pi d)}{\mathrm{i}(\omega_0 - n\omega) + \Gamma}. \tag{7}$$

The amplitude of the 1st harmonic is the largest in all the harmonics and is given by $M_+^{(1)} = \nu + \mathrm{i}\mu$ with

$$\nu = \frac{M_0 R_0 d\Gamma \sin c(\pi d)}{\Delta^2 + \Gamma^2}, \tag{8}$$

$$\mu = -\frac{M_0 R_0 d\Delta \sin c(\pi d)}{\Delta^2 + \Gamma^2}, \tag{9}$$

and

$$\left|M_+^{(1)}\right| = \frac{M_0 R_0 d \sin c(\pi d)}{\sqrt{\Delta^2 + \Gamma^2}}, \tag{10}$$

where $\Delta = \omega_0 - \omega$ is the detuning between the modulation frequency and the Larmor frequency. The line shapes of ν and μ are, respectively, absorptive and dispersive Lorentzian profiles each with half-width at half-maximum (HWHM) equal to Γ. Using Eqs. (1) and (6), the 1st harmonic components of the transverse MDMs are given by

$$\begin{aligned} M_x^{(1)} &= \mu\cos\omega t - \nu\sin\omega t, \\ M_y^{(1)} &= \nu\cos\omega t - \mu\sin\omega t. \end{aligned} \tag{11}$$

Experimentally, ν and μ are measured by phase sensitive detection of either M_x or M_y referenced to the in-phase or quadrature component of the 1st harmonic of the modulation frequency ω. The dispersive line shape of μ is particularly useful for operating magnetometers, since it can be used to generate feedback signals to lock the modulation frequency to the Larmor frequency.

The precession of the transverse MDM is detected by paramagnetic Faraday rotation. When a linearly polarized nearresonant probe beam propagates through an atomic vapor with a finite MDM along the beam direction, its polarization plane is rotated due to the circular birefringence of the vapor.[19] If the detuning of the probe from the optical transition resonance is much larger than the linewidth of the transition, in the case of y-propagating probe, the rotation angle is proportional to M_y, and quadrature component of its 1st harmonics ϕ is proportional to μ,[22] i.e.,

$$\phi = \frac{\sigma_0 nl}{2\Delta_{\mathrm{E}}}\mu \equiv \beta\mu, \tag{12}$$

where Δ_E is the detuning from the optical electronic transition, σ_0 is the absorption cross section of the optical transition at resonance, n is the atomic number density and l is the length of the atomic vapor along the probe direction. The sensitivity δB of the magnetometer is given by

$$\delta B = \frac{\delta\phi/\gamma}{\partial\phi/\partial\omega_0} = \frac{\delta\phi/\gamma\beta}{\partial\mu/\partial\Delta}, \tag{13}$$

where $\delta\phi$ is the noise of ϕ and $\partial\mu/\partial\Delta$ is the signal response to the field change. For constants γ and β, the best sensitivity can be achieved by minimizing $\delta\phi/(\partial\mu/\partial\Delta)$. We first analyze the effects of the duty cycle and the pumping rate on $\partial\mu/\partial\Delta$ or $|\partial\mu/\partial\Delta|$ which is named field response. According to Eq. (9), the maximum value of $|\partial\mu/\partial\Delta|$ is obtained at $\Delta = 0$, and this resonant field response will be denoted by k_0 and expressed as

$$k_0 = \left|\frac{\partial\mu}{\partial\Delta}\right|_{\Delta=0} = \frac{M_0 R_0 d \sin c(\pi d)}{(\Gamma_2 + R_0 d)^2} = \frac{2\mu_{\max}}{\Gamma}, \tag{14}$$

where $\mu_{\max}$=$M_0 R_0 d \sin c(\pi d)/2\Gamma$ represents the amplitude of the signal Eq. (9). For a fixed d, the maximum value of k_0 is achieved when $R_0 d = \Gamma_2$ and is given by

$$k_0^{\max}(d) = M_0 \mathrm{sinc}(\pi d)/4\Gamma_2 \tag{15}$$

Obviously when $d \to 0$, $k_0^{\max}(d)$ approaches to its ultimate limit $k_0^{\mathrm{Lim}} = M_0/4\Gamma_2$, which is $\pi/2$ times larger than $k_0^{\max}(d = 0.5)$. The dependences of k_0 on the average pumping rate R_0 for various duty cycles are plotted in Fig. 1. It shows that for any fixed duty cycle, the maximum field response $k_0^{\max}(d)$ is always obtained when the pumping rate is set at $R_0 d = \Gamma_2$. However, the smaller the duty cycle the larger the $k_0^{\max}(d)$ is.

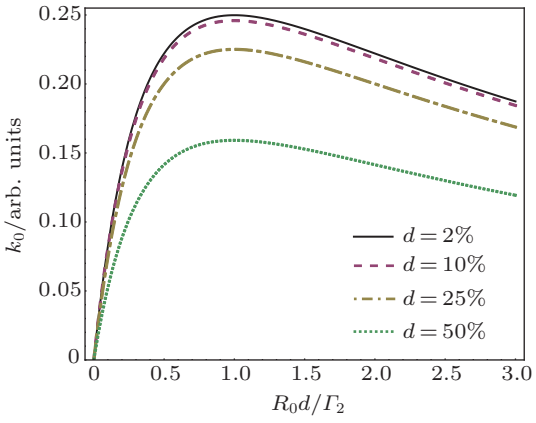


Fig. 1. (color online) Dependences of the resonant response k_0 on average pumping rate $R_0 d$ for various duty cycles. The solid, dash, dash-dot, and dot lines are for $d = 2\%$, 10%, 25%, and 50%, respectively.

For a fixed R_0, the maximum value of k_0 achievable by varying d, which we denote by $k_0^{\max}(R_0)$, is obtained when $\cot(\pi d) = 2R_0/\pi\Gamma$. The dependences of k_0 on d for various pumping rates are plotted in Fig. 2. It shows that $k_0^{\max}(R_0)$ increases with pumping rate and approaches to the ultimate limit k_0^{Lim}, when $R_0 \gg \Gamma_2$ and $R_0 d = \Gamma_2$. We can see that for practical purpose, by choosing $R_0 \sim 10\Gamma_2$ and $d \sim 10\%$, one can obtain a field response larger than $0.95 k_0^{\mathrm{Lim}}$.

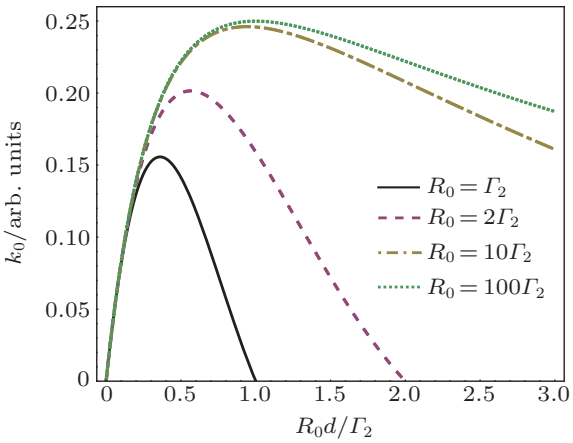


Fig. 2. (color online) Dependences of the resonant response k_0 on average pumping rate $R_0 d$ for various pumping rates. The solid, dash, dash-dot and dot lines are for $R_0 = \Gamma_2$, $2\Gamma_2$, $10\Gamma_2$, and $100\Gamma_2$, respectively.

It is interesting to compare the result of square-wave AM with that of sinusoidal AM where $R(t) = R_0 + R_0 \cos(\omega t)$. One can find that for sinusoidal AM, the maximum field response is obtained at $R_0 = \Gamma_2$ and is equal to $M_0/8\Gamma_2$, which is only half of the k_0^{Lim} for square-wave AM.

After having studied the effect of pumping on the field response, we turn to its effect on the noise. The noise $\delta\phi$ is generally contributed by the photon shot noise of the probe beam, the spin projection noise of the atoms, light shift back-action noise and other technical noises.[19] Here we only consider the possible noise related to the pumping parameters. Since β is independent of the pumping parameters, we have

$$\delta\phi = \beta\delta\mu \tag{16}$$

To study the noise of μ due to fluctuation of pumping rate, we differentiate Eq. (9) with respect to R_0 using Eq. (4) and obtain

$$\delta\mu_R = M_0\Delta \frac{\sin(\pi d)\left(R_0^2 d^2 - \Gamma_2^2 - \Delta^2\right)}{\pi(R_0 d + \Gamma_2)^4}\delta R_0. \tag{17}$$

It seems that $\delta\mu_R$ can be made arbitrarily small by letting $d \to 0$. However in reality, the fluctuation of pumping rate δR_0 is most likely to be proportional to R_0, so it is more practical to use the relative fluctuation of pumping rate $\delta R_0/R_0$, thus

$$\delta\mu_R = M_0\Delta \frac{R_0 \sin(\pi d)\left(R_0^2 d^2 - \Gamma_2^2 - \Delta^2\right)}{\pi(R_0 d + \Gamma_2)^4}\frac{\delta R_0}{R_0}. \tag{18}$$

Because BBM operates at resonance where $\Delta = 0$, $\delta\mu_R$ is insensitive to the relative fluctuation of pump rate. What if Δ is not exactly zero? At first glance, it seems that $\delta\mu_R \propto 1/R_0$ for large R_0. But it will not improve the sensitivity anymore

once $\delta\mu_R$ is smaller than the fundamental noise, such as spin projection noise $\delta\mu_{\rm sp}$ given by

$$\frac{\delta\mu_{\rm sp}}{M_0} \approx \sqrt{\frac{\Gamma}{N_{\rm A}}}, \tag{19}$$

where $N_{\rm A}$ is the number of atoms being detected. On the other hand, under the condition of maximum field response $R_0 d = \Gamma_2 = \Gamma/2$ and $d \ll 1$, we have

$$\frac{\delta\mu_R}{M_0} \approx \frac{\Delta^3}{2\Gamma^3}\frac{\delta R_0}{R_0}. \tag{20}$$

We will show that under our experimental conditions the above noise is already smaller than the spin projection noise $\delta\mu_{\rm sp}$.

Similarly, we can derive the noise of μ due to fluctuation of the duty cycle. Keep in mind that, in practice, δd is usually independent of d. Assuming $\Delta \ll \Gamma$, we have

$$\delta\mu_d \approx M_0 \Delta R_0 \frac{2R_0 d\,\mathrm{sinc}(\pi d) - \cos(\pi d)(R_0 d + \Gamma_2)}{(R_0 d + \Gamma_2)^3}\delta d. \tag{21}$$

One can see that $\delta\mu_d$ is also insensitive to the fluctuation of d at resonance. In the case of $\Delta \neq 0$, $\delta\mu_d$ is also proportional to $1/R_0$ for large R_0. However, when $R_0 d = \Gamma_2 = \Gamma/2$ and $d \ll 1$, we have

$$\begin{aligned}\frac{\delta\mu_d}{M_0} &\approx R_0\Delta\left[\frac{\pi^2 d^2}{3\Gamma^2} + O(d)^4\right]\delta d \\ &\approx d\frac{\pi^2\Delta}{6\Gamma}\delta d.\end{aligned} \tag{22}$$

We see that $\delta\mu_d$ can be tuned down by d until it becomes negligible compared with other noises.

We conclude that because the dispersive signal μ is insensitive to the fluctuation of pumping parameters near resonance, pumping induced noises are usually smaller than other fundamental noises in practice. Thus the optimal pumping condition for the sensitivity of AM BBM is $R_0 d = \Gamma_2$ and $d \to 0$, where the resonant field response $|\partial\mu/\partial\Delta|_{\Delta=0}$ is maximized.

3. Experimental setup

To verify our theory we conducted the following experiment. The schematic design of the experimental setup is shown in Fig. 3. A 24 mm × 24 mm × 24 mm cubic Pyrex cell containing isotopically enriched Rb (99.5 at.% ^{87}Rb) was placed in a ceramic oven at room temperature. The inner wall of the cell was coated with Octadecyltrichlorosilane (OTS).[23] to reduce the wall relaxation. The cell was filled with 5 Torr (1 Torr = 1.33322×10^2 Pa) N_2 buffer gas to increase the optical pumping efficiency by velocity changing collisions and radiation quenching. The oven was mounted in a 4-layer cylindrical μ-metal shield. Three pairs of Helmholtz coils inside the shield provided a uniform magnetic field in the z direction. The inhomogeneity of the field was measured and negligible when the field strength was below 2 mGs (1 Gs = 10^{-4} T), which corresponds to a Larmor frequency of 1.4 kHz for the ^{87}Rb ground state. Our experiments were performed at a Larmor frequency of 1181 Hz. Two 795-nm distributed feedback (DFB) lasers resonant with the $F = 1 \to F' = 2$ and $F = 2 \to F' = 2$ transitions were combined into a single pump beam propagating along the x axis. The intensity of the pump beam was square-wave modulated by an acoustic optical modulator (AOM) controlled by a function generator. Neutral density filters are to be inserted behind the AOM to change the pump intensity, hence R_0. The pump beam was circularly polarized by a linear polarizer followed by a quarter-wave plate. Finally the beam was expanded to 2 cm in diameter to cover almost the entire cell. The intensities of the two DFB lasers were adjusted to be equal throughout the experiment to minimize the hyperfine polarization. An external cavity diode laser (ECDL) traversing the cell in the y direction served as a probe beam. The probe frequency was red-detuned about 2.5 GHz from $F = 2 \to F' = 2$ resonance. We used such a large detuning, which is about 10 times the optical Doppler half width, in order to avoid any complication caused by the absorption of the probe light. The beam diameter and the power of the probe was 2 mm and 6 μW respectively. The PFR of the probe transmission was detected using a balanced photo-detector behind a Walleston prism, whose homodyne output was fed separately into a spectrum analyzer and a lock-in amplifier referenced to the AOM modulation. The dispersive signal of PFR was obtained from the lock-in amplifier with a 3-ms time constant by scanning the modulation frequency over 400 Hz across the resonance in 4 s.

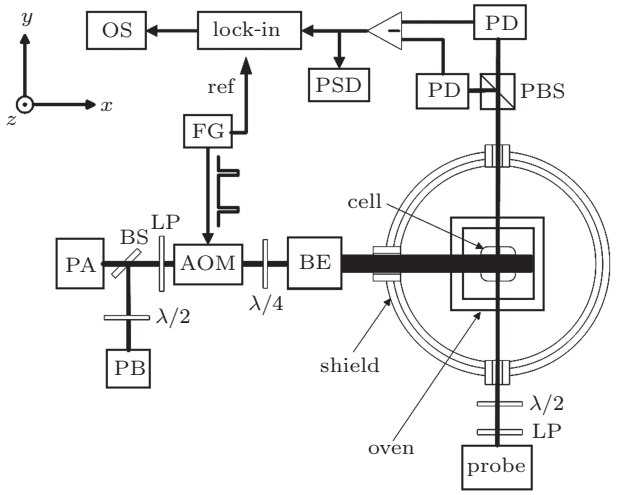


Fig. 3. Experimental setup. PA, PB: DFB lasers resonant with ^{87}Rb D1 $F = 2 \to F' = 2$ and $F = 1 \to F' = 2$ transitions respectively, BS: beam splitter, LP: linear polarizer, AOM: acousto-optic modulator, $\lambda/4$: quarter-wave plate, $\lambda/2$: half wave plate, BE: beam expander, Shield: magnetic shield composed of four layers of mu-metal, Probe: probe laser, PBS: polarizing beam splitter, PD: photon detector, Lock-in: lock-in amplifier, FG: function generator, ref: AOM modulation trigger signal for lock-in reference, PSD: spectrum analyzer for power spectral density, OS: digital oscilloscope.

4. Results and discussion

Figure 4 shows two typical PFR signals obtained in the experiment along with their fittings using Eq. (9). The pump power is 4.2 mW and duty cycles are 1.2% and 0.03%, respectively. One can see that the fitting to the data of the larger duty cycle is not so good as that of the smaller one. It is a general trend of our data that the line shape of the signal deviates from the pure Lorentzian profile of Eq. (9) when $R_0 d$ approaches to Γ_2, and becomes more distorted with increasing $R_0 d$, the reason for which will be discussed later.

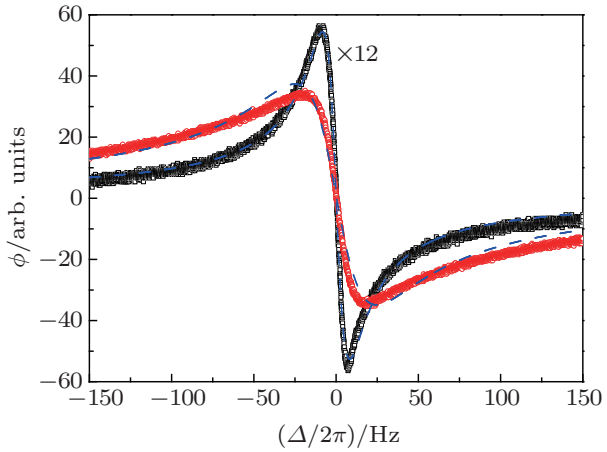


Fig. 4. (color online) The experimental field response signals of Faraday rotation and their fittings using Eq. (9). The pump light intensity is 4.2 mW. The black squares and red circles represent the data for duty cycles of 0.03% and 1.2%, respectively, the former is amplified by a factor of 12 for easy viewing. Blue dash lines represent the fittings.

The dependences of the linewidth Γ on duty cycle for various pumping rates are measured and plotted in Fig. 5. The value of Γ is given by half the peak-to-peak frequency gap directly measured from the dispersive signal. The vertical intercept and the slope of the linear fit represent the fitted values of Γ_2 and R_0 respectively. Since our experiments were performed at room temperature where $\Gamma_{\rm SE}$ is less than 0.15 $\rm s^{-1}$,[24] the Γ_2 is mostly contributed by wall relaxation rate $\Gamma_{\rm W}$.

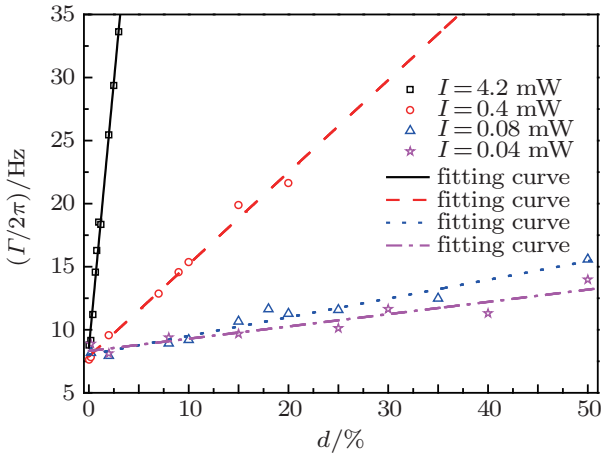


Fig. 5. (color online) Experimental dependences of the linewidth on duty cycle for various pump powers. Blocks, circles, triangles and stars represent data taken under total pump powers of 4.2 mW, 0.4 mW, 0.08 mW, and 0.04 mW, respectively.

Figure 6 shows the dependences of the resonant response k_0 on duty cycle for the same set of data presented in Fig. 5. The resonant response is obtained from the slope of a linear fit of 100 data points near the resonance center of the PFR signal. At the same time the power spectral density (PSD) at resonance, measured by the spectrum analyzer, shows that the noise floor near resonant frequency is constant within several percents and independent of the duty cycle. Using the actual experimental condition: $\Gamma_2 \approx 10\ 2\pi\cdot$Hz, $R_0 = 10\Gamma_2$, $d = 10\%$, $\Gamma \approx 20\ 2\pi\cdot$Hz, $N_{\rm A} = 10^{11}$ and assuming some large fluctuations of the detuning, duty cycle and pumping rate: $\Delta = 1\ 2\pi\cdot$Hz, $\delta d = 10^{-4}/\sqrt{\rm Hz}$, $\delta R_0/R_0 = 10^{-3}/\sqrt{\rm Hz}$, we can estimate that the pumping parameter related noises given by Eqs. (20) and (22) are smaller than the spin projection noise given by Eq. (19). By checking the probe intensity dependence of the same PSD, we find that the signal-to-noise ratio is proportional to the square root of the probe intensity, indicating that our system is actually limited by the photon shot noise of the probe.

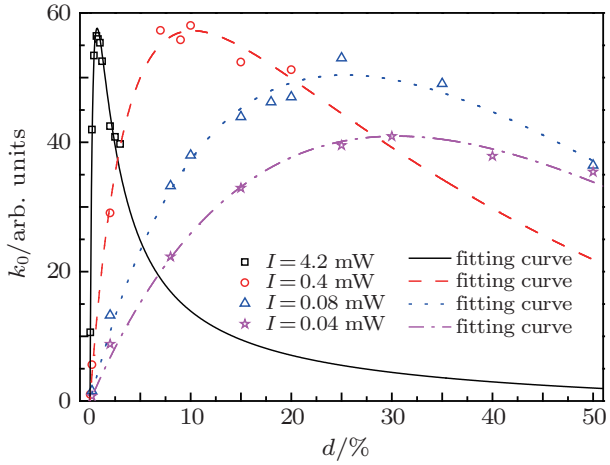


Fig. 6. (color online) Dependences of the resonant response on duty cycle for various pump powers. Blocks, circles, triangles and stars represent experimental data taken under total pump powers of 4.2 mW, 0.4 mW, 0.08 mW, and 0.04 mW, respectively.

The fitted pumping rate and the optimal duty cycle obtained from the fittings are listed in Table 1. Notice that there is a discrepancy between the pumping rate obtained by fitting the duty cycle dependence of the linewidth and the resonant field response. Theoretically k_0 is related to Γ by Eq. (14). However when the average pumping rate exceeds the relaxation rate in the dark this relation will not hold exactly due to the hyperfine pumping effect. In our experiment, the probe beam is set to observe the MDM on the $F = 2$ hyperfine sublet mainly. However, inevitable hyperfine pumping will increase the population on the $F = 2$ sublet, causing M_0 to increase with increasing duty cycle, while in the current theory M_0 is assumed to be a constant. Such an effect causes the fitted pumping rate R_k to be bigger than R_Γ.

Table 1. Fitting parameters of the experimental data. I_P is the total pump intensity. R_Γ and Γ_2 are respectively the R_0 and the Γ_2 obtained by fitting the data in Fig. 5. R_k and d_k are respectively the R_0 and the optimal duty cycle for $k_0^{\max}(d)$ obtained by fitting the data in Fig. 6.

I_P/mW	$(\Gamma_2/2\pi)$/Hz	R_Γ/Γ_2	d_k/%	R_k/Γ_2
4.2	8.6 ± 0.4	98 ± 8	0.7	142 ± 6
0.4	7.9 ± 0.3	9.3 ± 0.7	10	9.1 ± 0.5
0.08	8.0 ± 0.3	1.8 ± 0.2	25	2.5 ± 0.2
0.04	8.3 ± 0.4	1.2 ± 0.2	30	1.7 ± 0.1

Large average pumping rate also causes a deviation of the experimental signal line shape from the pure dispersive Lorentzian profile given by Eq. (9) as can be seen clearly from the signal of the large pump intensity in Fig. 4. Since both the duty cycle and pumping rate are fixed in this case, this discrepancy cannot be explained by the reason as mentioned above. By tracing back the derivation of Eq. (9), we suspect that Eq. (5) is no longer accurate for describing the dynamics of MDM, because it might neglect some effect which is important at high average pumping rate. One possibility is the coupling between the evolutions of different spin polarization moments. For atoms with spin quantum number F, the circularly polarized pump light can generate spin polarization moments (PMs) of all ranks $\kappa = 0, 1, 2, \ldots, 2F$.[25] The precession frequency of a transverse PM of rank κ is equal to $\kappa\omega_0$, so PMs of $\kappa \geq 1$ are all synchronously pumped when the light modulation frequency matches the Larmor frequency ω_0. A weak probe can only detect PMs of $\kappa = 0, 1, 2$, which are named population, orientation and alignment respectively.[25] The magnetic dipole moment probed by PFR at far optical detuning is only proportional to the orientation. For isotropic relaxations, PM of each rank evolves independently, but if the relaxation is anisotropic, PM's of different ranks might couple to each other.[26,27] Since the power broadening relaxation is anisotropic, it can cause couplings of PMs. For weak pumping, the magnitudes of higher rank PMs are negligible and the dynamics of orientation can be treated independently as described in Eq. (5). But when the average pumping rate exceeds Γ_2, the higher rank PMs become significant, and their coupling with the orientation might cause the deviation of its signal from a pure Lorentzian.

5. Conclusions

We theoretically study the dependences of the line shape of a square-wave amplitude-modulated Bell–Bloom magnetometer on the intensity and duty cycle of the pump light. We show that the maximum field response of the magnetometer can be achieved at the resonance center of the dispersive parametric-Faraday-rotation signal together on the condition that the duty cycle is small and the average pumping rate is approximately equal to the transverse relaxation rate in the dark Γ_2. The theoretical results are in agreement with experimental results for pumping rates ranging over two orders of magnitude above Γ_2. We also show that the signal at resonance is insensitive to the fluctuations of pumping rate and duty cycle. Thus it is the same condition for both the maximum field response and the optimal sensitivity. The line shape of experimental signal starts to deviate from the prediction of the theory when the average pumping rate exceeds Γ_2. A full density matrix calculation, which includes the hyperfine pumping and the dynamics of higher rank polarization moments is expected to give a more accurate description of this phenomenon.

Acknowledgment

We thank Martin Schaden for reading the manuscript.

References

[1] Bell W E and Bloom A L 1961 *Phys. Rev. Lett.* **6** 280
[2] Bell W E and Bloom A L 1961 *Phys. Rev. Lett.* **6** 623
[3] Alexandrov E B, Auzinsh M, Budker D, Kimball D F, Rochester S M and Yashchuk V V 2005 *J. Opt. Soc. Am. B* **22** 7
[4] Budker D and Romalis M 2007 *Nat. Phys.* **3** 227
[5] Gawlik W, Krzemien L, Pustelny S, Sangla D, Zachorowski J, Graf M, Sushkov A O and Budker D 2006 *Appl. Phys. Lett.* **88** 131108
[6] Huang H C, Dong H F, Hao H J and Hu X Y 2015 *Chin. Phys. Lett.* **32** 098503
[7] Zhang J H, Liu Q, Zeng X J, Li J X and Sun W M 2012 *Chin. Phys. Lett.* **29** 068501
[8] Budker D, Kimball D F, Yashchuk V V and Zolotorev M 2002 *Phys. Rev. A* **65** 055403
[9] Jimenez-Martinez R, Griffith W C, Wang Y J, Knappe S, Kitching J, Smith K and Prouty M D 2010 *IEEE Trans. Instrum. Meas.* **59** 372
[10] Ben-Kish A and Romalis M V 2010 *Phys. Rev. Lett.* **105** 19
[11] Fescenko I, Knowles P, Weis A and Breschi E 2013 *Opt. Express* **21** 15121
[12] Breschi E, Gruijc Z D, Knowles P and Weis A 2013 *Phys. Rev. A* **88** 2
[13] Budker D, Kimball D F, Rochester S M, Yashchuk V V and Zolotorev M 2000 *Phys. Rev. A* **62** 043403/1
[14] Pustelny S, Kimball D F J, Rochester S M, Yashchuk V V, Gawlik W and Budker D 2006 *Phys. Rev. A* **73** 023817
[15] Pustelny S, Wojciechowski A, Gring M, Kotyrba M, Zachorowski J and Gawlik W 2008 *J. Appl. Phys.* **103** 7
[16] Schultze V, Ijsselsteijn R, Scholtes T, Woetzel S and Meyer H G 2012 *Opt. Express* **20** 28056
[17] Grujic Z D and Weis A 2013 *Phys. Rev. A* **88** 11
[18] Jimenez-Martinez R, Griffith W C, Knappe S, Kitching J and Prouty M 2012 *J. Opt. Soc. Am. B* **29** 3398
[19] Budker D and Kimball D F 2013 *Optical magnetometry* (New York: Cambridge University Press)
[20] Graf M T, Kimball D F, Rochester S M, Kerner K, Wong C, Budker D, Alexandrov E B, Balabas M V and Yashchuk V V 2005 *Phys. Rev. A* **72** 23401
[21] Wackerle G, Appelt S and Mehring M 1991 *Phys. Rev. A* **43** 242
[22] Savukov I M, Seltzer S J, Romalis M V and Sauer K L 2005 *Phys. Rev. Lett.* **95** 063004
[23] Zhang G, Wei L, Wang M and Zhao K 2015 *J. Appl. Phys.* **117** 043106
[24] Happer W and Tam A C 1977 *Phys. Rev. A* **16** 1877
[25] Happer W 1972 *Rev. Mod. Phys.* **44** 169
[26] Happer W 1970 *Phys. Rev. B* **1** 2203
[27] Bernabeu E and Tornos J 1985 *Nuovo Cimento D* **5** 315